



# Forest Characterization Using C-band SAR Data—Initial Results of EOS-04 Data

Jayant Singhal<sup>1</sup>  · Tanumi Kumar<sup>2</sup> · Rakesh Fararoda<sup>3</sup> · Prabir Kumar Das<sup>2</sup> · Rakesh Paliwal<sup>3</sup> · Sudhakar Reddy Chintala<sup>4</sup> · Gopalakrishnan Rajashekar<sup>4</sup>

Received: 20 June 2023 / Accepted: 10 November 2023 / Published online: 16 December 2023  
© Indian Society of Remote Sensing 2023

## Abstract

In satellite remote sensing, C-band synthetic aperture radar (SAR) sensors with the frequency of about 5.4 GHz and wavelength of about 5.5 cm interact heavily with the leaves, twigs and small stems. Hence, it is ideal for monitoring vegetation phenology, stratification of canopy closure/openness and biomass assessment of low- to medium-aboveground-biomass (AGB) density regions. Earth Observation Satellite-04 (EOS-04) is a C-band SAR mission from the Indian Space Research Organisation launched on 14 February 2022. This study presents the applications of EOS-04 data in forest phenological studies and biomass estimation in different vegetation conditions. Multi-temporal EOS-04 data were used to track the land surface phenology of tropical dry deciduous forests of Betul, Madhya Pradesh, which is mostly dominated by *Tectona grandis*. Phenological metrics were also derived from the tracked land surface phenology. For the mangrove forests of Sundarbans delta for two islands, namely Lothian and Dhanchi characterization in terms of canopy density and homogeneity/heterogeneity was carried out and AGB was estimated. The AGB values ranged from 29 to 241 Mg/ha, and the validation root mean square error (RMSE) was calculated to be 34 Mg/ha. EOS04 data were also used in combination with L-band ALOS PALSAR data for the forest biomass estimation in the part of Central India. Synergistic utilization of C- and L-band improves upon the individual models in terms of  $R^2$  and RMSE. L-band HV backscatter estimates AGB with a correlation coefficient of 0.49 which improved to 0.57 with the inclusion of C-band and estimates AGB with RMSE of 29 Mg/ha. This study successfully demonstrated the usability of EOS-04 for tracking land surface phenology and deriving phenological metrics from it, for the characterization of mangrove forests and its AGB estimation and for AGB estimation of forests in low-biomass regions.

**Keywords** EOS-04 · C-band · SAR · Phenology · Biomass · Mangroves

## Introduction

Forests are important as they hold about 45% of the terrestrial carbon in live aboveground biomass (Bonan, 2008). Forests hold more than 60,000 unique tree species and provide habitat for 68% of mammal species, 75% of bird species and 80% of amphibian species (The state of World's Forests, 2020). Remote sensing has been a crucial tool for monitoring vegetation cover, vegetation structure, disturbances in forests, forest biodiversity and biomass (Lechner et al., 2020); however, the use of optical remote sensing data in cloud-prone tropical forest is challenging. SAR sensors have the ability to monitor vegetation through clouds and interact with different parts of the plants depending on the operating frequencies. C-band is designated for the portion of the electromagnetic spectrum in the microwave range from 4

✉ Jayant Singhal  
jayantsinghal@hotmail.com

- <sup>1</sup> Regional Remote Sensing Centre – North, National Remote Sensing Centre, Indian Space Research Organisation, Antariksh Bhavan, Plot No.7, Planning Area Center, Sadiq Nagar, New Delhi 1100049, India
- <sup>2</sup> Regional Remote Sensing Centre – East, National Remote Sensing Centre, Indian Space Research Organisation, BG-2, Action Area – 1B, New Town, Kolkata 700 163, India
- <sup>3</sup> Regional Remote Sensing Centre – West, National Remote Sensing Centre, Indian Space Research Organisation, New Town, New ISRO Complex, Jodhpur 342 005, India
- <sup>4</sup> Forestry and Ecology Group, Remote Sensing Applications Area, National Remote Sensing Centre, Indian Space Research Organisation, Balanagar, Hyderabad 500037, India

to 8 GHz (Peebles, 1998). C-band SAR satellites mostly work at about 5.4 GHz (RADARSAT-2, Sentinel-1, RISAT-1, etc.). EOS-04 is a C-band (5.4 GHz) SAR satellite mission launched by ISRO on 14 February 2022 which has full polarimetric capabilities. It is a successor to the RISAT-1 satellite with a similar configuration. EOS-04 SAR payload operates in C-band frequency (5.4 GHz) with capability to image in multiple resolutions in single, dual, circular or full polarization. Main feature of the mission is that the satellite performs undisturbed systematic acquisition of data in descending passes in medium resolution scanSAR (MRS) mode and reserves scanning in fine resolution stripmap (FRS) mode for ascending passes for user-requested sites. So, the same satellite can be used for time series analysis of a target area at medium resolution; high-resolution backscatter images can be captured for mapping and delineation-related studies.

In forest ecosystems, especially in deciduous forests, the onset of leaves, colouration, fall of leaves ('leaf senescence') mark the start and the end of the photosynthetically active period. Therefore, phenology plays a major role in the productivity and carbon storage activity of the forest ecosystem (Richardson et al., 2010). Phenological information in terms of multi-temporal satellite data has also been used to map tree communities present in forests (Mishra et al., 2021). Historically, these events that mark different stages of phenological cycles were recorded by people in situ in the field which was a very time-consuming and laborious process and the records were subjective to the field personnel taking it (Schaber & Badeck, 2002). Then, these events were recorded using field instruments like Phenocam (Brown et al., 2016), RGB cameras and radiation sensors (Soudani et al., 2021). But these values recorded in the field by instruments or by human observations were very site specific and do not describe the spatial variations in the phenology of the forests. Spectral vegetation indices (SVI) generated from multi-spectral sensors present on satellites like Sentinel-2A and 2B (Misra et al., 2020), LANDSAT Series (Mas & Araújo, 2021), Suomi NPP (Zhang et al., 2018) and Indian remote sensing (IRS) (Garg et al., 2008). A series of satellites have been used to track the land surface phenology of the forests. But usage of data from optical sensors for land surface phenology-related applications is limited by the problem of cloud cover, especially during the monsoon season over India where a lot of the photosynthetic activity is happening. C-band SAR is sensitive to plant foliage and is not easily attenuated by cloud cover, and hence, it can be used to capture the complete year phenological cycle of forests. This study demonstrated the ability of EOS-04 C-band data to do the same and also derive phenological metrics from it.

Mangrove forests are considered to be one of the vital coastal ecosystems that continue to be threatened by both natural and anthropogenic factors. The Sundarbans

mangrove forests are located in the Bay of Bengal delta created by the confluence of the Ganges, Brahmaputra and Meghna rivers. The Indian part of the Sundarbans extends across the districts of South 24 Parganas and North 24 Parganas of West Bengal State in India ([http://www.sundarbanbiosphere.org/html\\_files/flora.htm](http://www.sundarbanbiosphere.org/html_files/flora.htm)). A summary of studies on radar remote sensing was reviewed in the field of mangroves by Proisy et al. (2001). However, the application of C-band SAR for quantifying forest canopy density has not been satisfactorily understood. When analysing SAR images to distinguish between different types of forest cover, texture transforms are crucial (Nelson et al., 2006). In comparison with VV-polarized light energy, studies have demonstrated that a greater part of HH-polarized microwave energy can pass through the forest canopy and reach the ground surface, where tidal inundation has a significant impact on scattering and reflection (Wang et al., 1995). In C band SAR data, the HV-polarized component plays an important role in volume scattering and is extensively used in forest canopy density studies. On surveying the studies, it is found that reports on to the characterization of Indian mangrove forests in terms of canopy density using C-band SAR data are minimal. Besides, biomass estimation of the Indian Sundarbans forests using C-band SAR data is almost lacking. This study demonstrated that using EOS-04 C-band SAR data, mangrove forests can be characterized in terms of canopy density and their AGB can be estimated spatially.

Along with forest mapping, phenological studies, the quantification of vegetation carbon has received much attention as it directly impacts the inventory of greenhouse gases, considered one of the primary causes of climate change (Gibbs et al., 2007). Nearly 80% of the aboveground carbon is stored by the forests in the form of biomass (Solomon, 2007). Forest ecosystems are excellent sink of CO<sub>2</sub>, and they mop up CO<sub>2</sub> from the atmosphere and store it in the form of biomass through the process of photosynthesis (Wani et al., 2012). Accurate information on biomass stock and its spatial distribution and change dynamics is therefore essential to plan adaptation and mitigation actions in the land-use sector. Remote sensing technology and its datasets (both optical and radar) have been extensively used for biomass estimation (Rajashekar et al., 2018; Rakesh et al., 2021; Reddy et al., 2017; Thumaty et al., 2016). Forest biomass is stored in multiple vertical stories and microwave is able to penetrate deeper into forest canopies depending on operating frequencies and provide information about stored woody biomass. The radar backscatter increases with increasing forest AGB from low to medium levels, but gradually loses its sensitivity to higher levels of AGB and asymptotes to a saturation level, resulting in a logarithmic or sigmoidal relationship between AGB and backscatter, according to previous studies (Hayashi et al., 2019; Mermoz et al., 2015). C-band being about 5.5 cm interacts mainly with leaves and small twigs

and is therefore sensitive towards low- to medium-AGB regions. L-band with 24 cm wavelength is much more sensitive towards medium-AGB regions. Considering the vegetation interaction of C- and L-band, synergistic utilization of both to improve the biomass estimation in low–medium-biomass regions was tested in this study.

Considering the importance of the SAR data for vegetation studies and systematic availability of the EOS-04 data, the present study focuses on the utilization of C-band EOS-04 data in (1) forest phenological studies, (2) mangrove characterization in terms of canopy density and heterogeneity/homogeneity and (3) forest biomass estimation. Three ideal study sites of the three different objectives were selected in order to showcase the EOS-04 application for forest studies over India.

## Study Site

### Land Surface Phenology Tracking Study

A part of forested region near Betul, Madhya Pradesh, was used as the study site for monitoring the land surface phenology of the region. The study site extended from 77.3978 to 77.4553°E and from 21.8350 to 21.8897°N, about 6km × 6km region consisting mostly of forests. Forests here are mostly dry deciduous type (ideal for tracking land surface phenology) and dominated by teak (*Tectona grandis*). Figure 1 shows the location of the site in the state of Madhya Pradesh. A forest layer was developed from Reddy et al. (2015) by clubbing all the forest classes together and is depicted in green colour in Fig. 1.

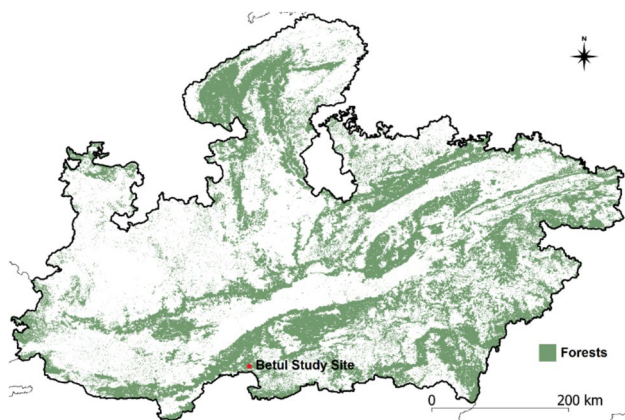


**Fig. 1** Location of study site near Betul, Madhya Pradesh, India. Forests are shown in green colour (Color figure online)

## Mangrove Characterization Study

The study area included the Lothian and Dhanchi Islands of Sundarbans, Lothian extending from 21° 36' N–88° 18' E to 21° 42' N–88° 21' E and Dhanchi extending from 21° 36' N–88° 25' E and 21° 43' N–88° 28' E (Fig. 2). The different mangrove communities present in these two islands are *Aegialitis–Excoecaria*, *Avicennia*, *Excoecaria*, mixed (*Ceriops–Excoecaria–Phoenix*), *Phoenix*, mixed mangroves, fringe mangrove communities, besides other eco-morphological classes (marsh vegetation, saline blank and beach vegetation) (Kumar et al., 2021).

## Aboveground Biomass Upscaling Study

The study was carried out in the part of Madhya Pradesh in the Khandwa district near the Indira Sagar dam. Forests in this region are dominated by teak (*Tectona grandis*), *Diospyros melanoxylon*, *Lagerstroemia parviflora* and *Madhuca longifolia*. Figure 3 shows the study area maps along with the RISAT image used in the study (HV—backscatter).

## Methodology

### Land Surface Phenology Tracking Study

All available EOS-04 data in MRS mode were acquired for the study site, i.e. 12 images from 27 March 2022 to 20 November 2022. The data were available for HH and HV polarization only. For this study, only HH images were used.

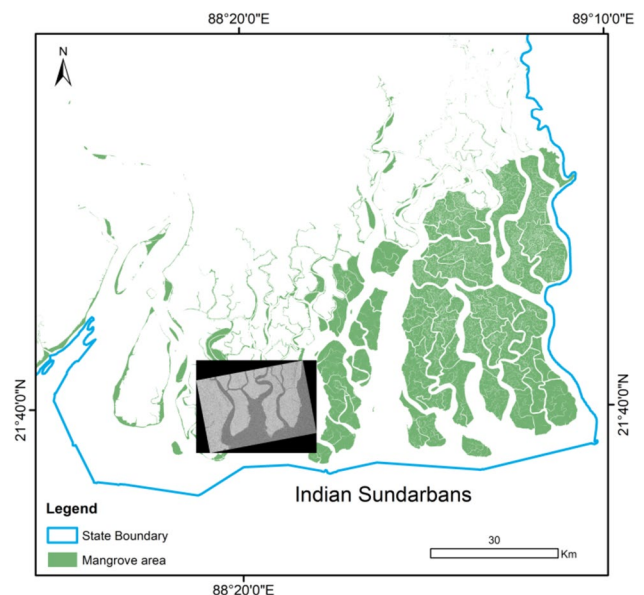


**Fig. 2** Index map of the study area with overlaid RISAT data

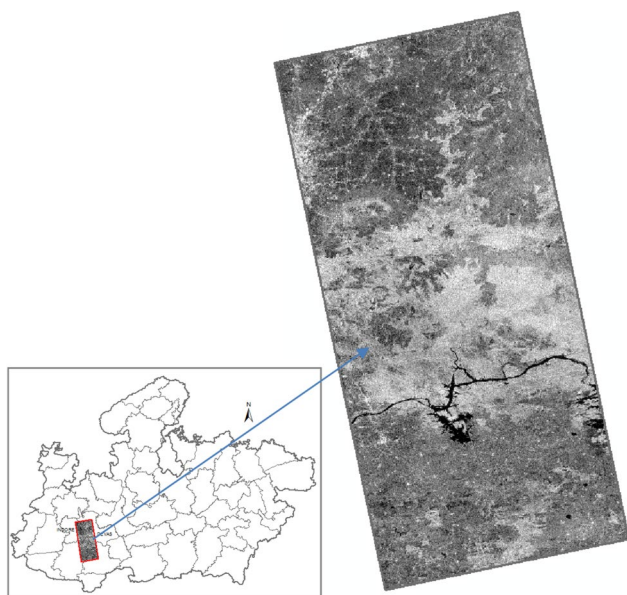


**Fig. 3** Location of study area on the map of Madhya Pradesh state of India

The images came with local incidence angle (LIA) images also. All the 12 images were converted from digital number values to sigma naught values. Taking the grid of the first image as the reference grid, all the other 11 images were resampled to align with the reference grid. The aligning of the raster was carried out in R using the ‘raster’ package. All the 12 images were stacked together to create a time series stack. The time series sigma naught values were then plotted for  $21^{\circ} 51' 46.84''$  N,  $77^{\circ} 25' 33.67''$  E (Fig. 4).

Phenological metrics were defined as follows from the plot:

#### 1. Maximum Foliage:

Maximum foliage is defined as the maximum back scatter sigma naught value received throughout the year.

#### 2. Time of Maximum Foliage

: Time of Maximum Foliage is defined as the date on which Maximum foliage value was noted in the time series stack.

#### 3. Leaf onset

: Leaf onset was defined as the backscatter value of the first local minimum in the time series stack before the event of maximum foliage occurs.

#### 4. Time of leaf onset:

Time of leaf onset was defined as the date on which Leaf onset occurs in the time series stack.

#### 5. Leaf offset

: Leaf offset was defined as the backscatter value of the first local minimum in the time series stack after the event of maximum foliage occurs.

#### 6. Time of leaf offset:

Time of leaf onset was defined as the date on which Leaf offset occurs in the time series stack.

The above-mentioned rules were applied (Fig. 5) for the entire image stack for the Betul study site.

## Mangrove Characterization Study

RISAT 1A Fine Resolution Stripmap 1 (FRS 1) having an incidence angle of  $39.76^{\circ}$  was utilized. Data acquired on 25 February 2022 of ascending mode were used. The data characteristics are given in Table 1.

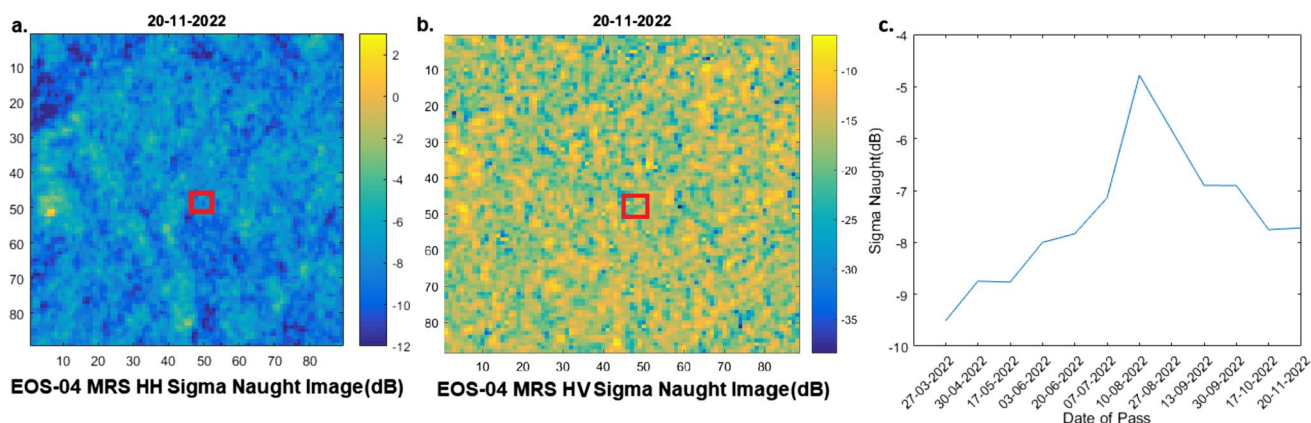


**Fig. 4** a EOS-04 MRS HH sigma naught image of the study site near Betul, Madhya Pradesh. b EOS-04 MRS HV sigma naught image of the study site. Red outline indicates the area of which time series sigma naught profile (HH only) is plotted in c (Color figure online)

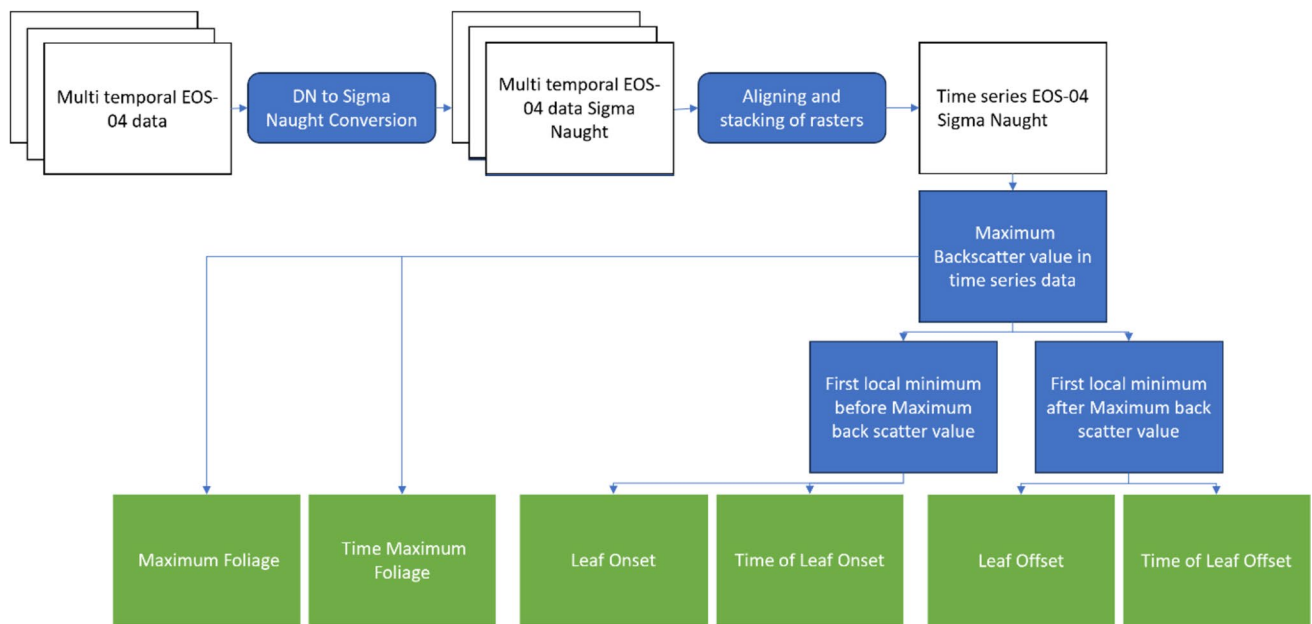


Fig. 5 Flowchart explaining the process to derive phenological metrics

Table 1 Data characteristics

| Data characteristics    |                      |
|-------------------------|----------------------|
| Imaging mode            | FRS 1                |
| Polarization            | Dual, HH, HV         |
| Date of pass            | 25th Feb 2022        |
| Product type            | L2A Enhanced Geotiff |
| Input resolution along  | 3.00 m               |
| Input resolution across | 2.16 m               |
| Line spacing            | 2.25 m               |
| Pixel spacing           | 2.25 m               |
| Node                    | Ascending            |
| Orientation             | Right                |
| Incidence angle         | 39.76 degrees        |

The SAR data processing involved downloading, calibration and speckle reduction. The calibration equation used was as follows:

$$\sigma^\circ = 10\log_{10}(\text{DN}^2) + 10\log_{10}(\sin i_p) - K_{\text{dB}} \quad (1)$$

where sigma naught (dB)—backscattering coefficient, DN—digital number,  $i_p$ —per pixel incidence angle and  $K_{\text{dB}}$ —calibration constant.

### Classification of the Forests Based on Canopy Closure/Density

Cross-polarization ratio (XPR) was computed using the back-scattering coefficients of HH and HV channels. Preliminary decision rules were developed using the XPR values and applied in the decision tree algorithm within the mangrove mask for classifying the mangroves into canopy closure/density classes.

### Characterization of the Mangrove Forests in Terms of Canopy Homogeneity/Heterogeneity

SAR data of forests are highly textured in nature. This textural property of SAR data was used to characterize mangrove forests. Grey-level co-occurrence matrix (GLCM) (Clausen, 2002) is a typical technique used for quantifying texture mathematically. GLCM were computed for  $25 \times 25$  windows of unfiltered HH images. In the current investigation, entropy and angular second moment were employed. Entropy (E) is used as a measure of heterogeneity, and angular second moment (ASM) is used as a measure of local homogeneity. Texture values were applied in the decision tree algorithm on the masked mangrove regions for the characterization of the mangroves.

## Estimation of Aboveground Biomass

**Field Measurements** A simple random sampling method was used as a ground truth sampling strategy for the measurement of biophysical attributes, such as basal girth, total tree height and canopy diameter of mangrove trees. Considering the mangrove community zonation maps (Ajai et al., 2012), a minimum of two quadrats was selected per class. Based on the accessibility into the forests, GPS-aided field visits were carried out for the Lothian and Dhanchi Islands for the collection of quadrat-level species information and biophysical attributes of mangrove trees.

### Calculation of Aboveground Biomass

AGB was calculated as the product of tree volume and wood density (Briggs, 1977). Two separate formulae were used for estimating tree volume—one for the computation of the volume of smaller trees (height  $\leq 3.9$  m) (Eq. 2) and the other for large trees (height  $> 3.9$  m) (Eq. 3)

$$\text{Volume} = \left\{ \pi \left( \frac{D^2}{4} \right) \times h \right\} \quad (2)$$

$$\text{Volume} = \left\{ \pi \left( \frac{D^2}{12} \right) \times h^3 \div (h - b)^2 \right\} \quad (3)$$

where  $b = 1.3$  m (Joshi & Ghose, 2014),  $D =$  diameter (m) at the base and  $h =$  height (m) of the plant. Instead of estimating wood density using a destructive sampling procedure, wood density data of mangrove species were collected from published works (Ilic et al., 2000; Joshi & Ghose, 2014; Martawijaya, 1992) and used in this study. AGB for each mangrove species was estimated as the product of the volume of that tree and the wood density of that species based on the equation as follows:

$$\text{AGB} = \text{Volume} \times \text{WD} \quad (4)$$

where AGB is the aboveground biomass and WD is the wood density of a particular mangrove species.

### Modelling of AGB of Forest Trees Using SAR Signatures and Field Observations and AGB Estimation

Stepwise linear multiple regression analyses were applied to express/represent AGB (dependent variable) in terms of independent variables like other biophysical parameter(s) and radar backscatter values of the two polarization(s). A

**Table 2** EOS-4 datasets used in the study

| Data characteristics    |                      |
|-------------------------|----------------------|
| Imaging mode            | MRS                  |
| Polarization            | Dual, HH, HV         |
| Date of pass            | 28 June 2022         |
| Product type            | L2A Enhanced Geotiff |
| Input resolution along  | 33.12 m              |
| Input resolution across | 17.27 m              |
| Line spacing            | 18 m                 |
| Pixel spacing           | 18 m                 |
| Node                    | Descending           |
| Orientation             | Right                |
| Incidence angle         | 37.79998 degrees     |
| Centre latitude         | 22.432741            |
| Centre longitude        | 76.376874            |

statistically significant model at the 0.05 level and with the highest  $R^2$  was selected and applied on the HH and HV channels of each of the mangrove community zonation rasters over the study area to obtain the per pixel AGB. Finally, AGB was calculated in megagram/hectare (Mg/ha) over the Lothian and Dhanchi Islands. The SAR-derived AGB values were validated using field-estimated AGB values.

## Aboveground Biomass Upscaling Study

### Data Used

EOS-04 data in MRS mode with HH and HV polarization acquired during June-2022 (Table 2) over the part of Madhya Pradesh were used for forest AGB estimation. SAR data were converted to sigma naught values using Eq. 1 speckle filtered to remove the speckle noise.

### Field Data

Ground inventory data from 26 plots of 0.1ha size were used for biomass estimation. Field-measured variables such as diameter, tree height and species scientific name were recorded during field inventory. Field inventory data are used from the National Field Inventory carried out as part of the National Carbon Project, Vegetation Carbon Pool Project phase-II during 2018–2019 under the ISRO-Geosphere Biosphere Programme. Forest Survey of India (FSI) developed

volumetric equations and these were used to estimate stem volume which was further converted to tree biomass using wood density and biomass expansion factors.

$$AGB = \text{Volume} \times \text{WD} \times \text{BEF} \quad (5)$$

where volume is estimated through volumetric equations developed by FSI, WD is wood density and BEF is biomass expansion factor.

Species specific volume equations were used for the volume equation database created by FSI (FSI, 1996), wood density data were used from the Indian Woods database (FRI, 1996) and biomass expansion factors were derived from Kaul et al. (2011).

### Modelling Forest AGB

Field-measured biomass values from 26 field plots were correlated with HH and HV backscatter values. SAR data were calibrated and processed for speckle filtering. Field-measured biomass values were regressed against HH and HV backscatter of C- and L-band SAR data. Finally, HV backscatter was used as it gives a better correlation coefficient. Multiple linear regression was also performed using C- and L-band HV backscatter data.

**Table 3** Derived phenological metrics and their mean and standard deviations for the study site

| Phenological metrics    | Mean            | Standard deviation |
|-------------------------|-----------------|--------------------|
| Leaf onset              | −9.9900 dB      | 1.6963 dB          |
| Maximum foliage         | −4.9980 dB      | 1.7923 dB          |
| Leaf offset             | −8.4729 dB      | 1.7121 dB          |
| Time of leaf onset      | 6 May 2022      | 26.37 days         |
| Time of maximum foliage | 28 August 2022  | 23.06 days         |
| Time of leaf offset     | 9-November 2022 | 22.05 days         |

## Results

### Land Surface Phenology Tracking Study

The phenological metrics as derived are shown in Fig. 6. Usually, the time of maximum foliage also corresponds to the peak monsoon season and hence under complete cloud cover. The method used here was able to get the complete phenological profile of the vegetation during the monsoon season, which is not possible with optical remote sensing data-driven spectral vegetation index-based methods.

For the study site, the average sigma naught at leaf onset was found to be −9.9900 dB with a standard deviation of

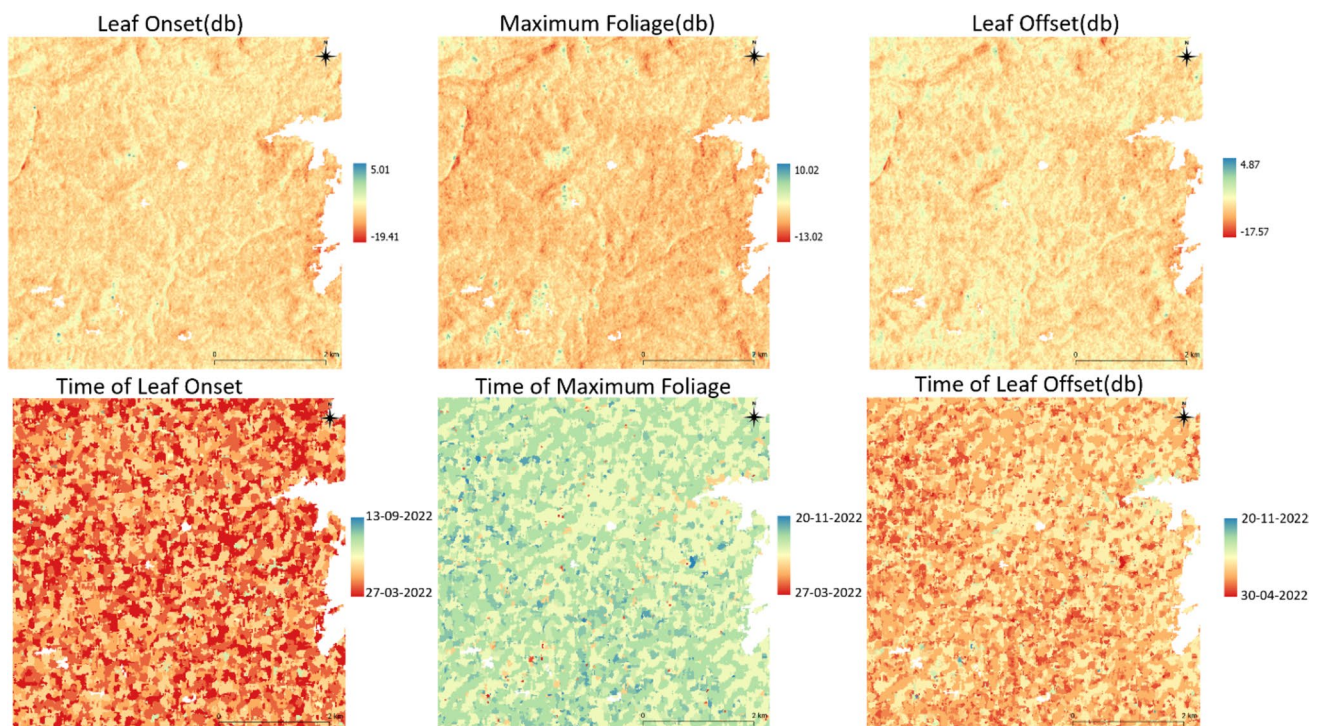


**Fig. 6** **a** Sigma naught values of the study site at the time of leaf onset, **b** maximum sigma naught values for the study site throughout the time series, **c** sigma naught values of the study site at the time of

leaf offset, **d** date of occurrence of leaf onset event, **e** date on which maximum foliage is achieved, **f** date of occurrence of leaf offset

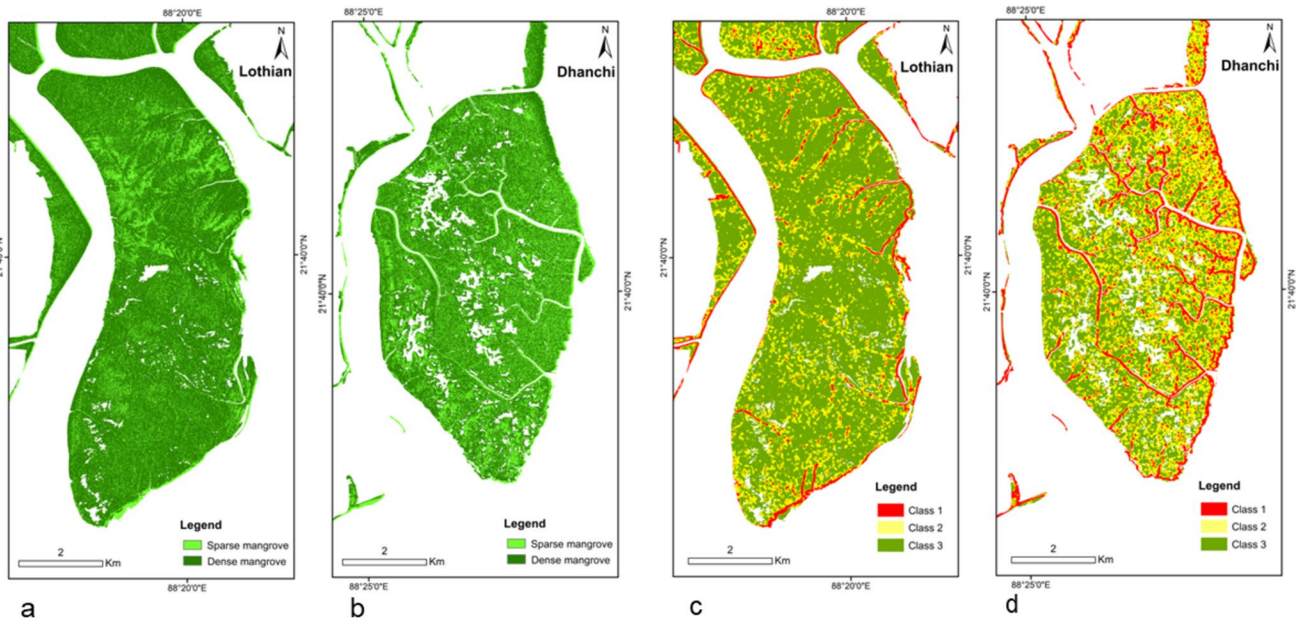


**Fig. 7** Preliminary classification using decision tree algorithms for mangrove forest density (a, b) and canopy homogeneity/heterogeneity (c, d) applied separately on the mask of mangrove region of Lothian and Dhanchi Islands



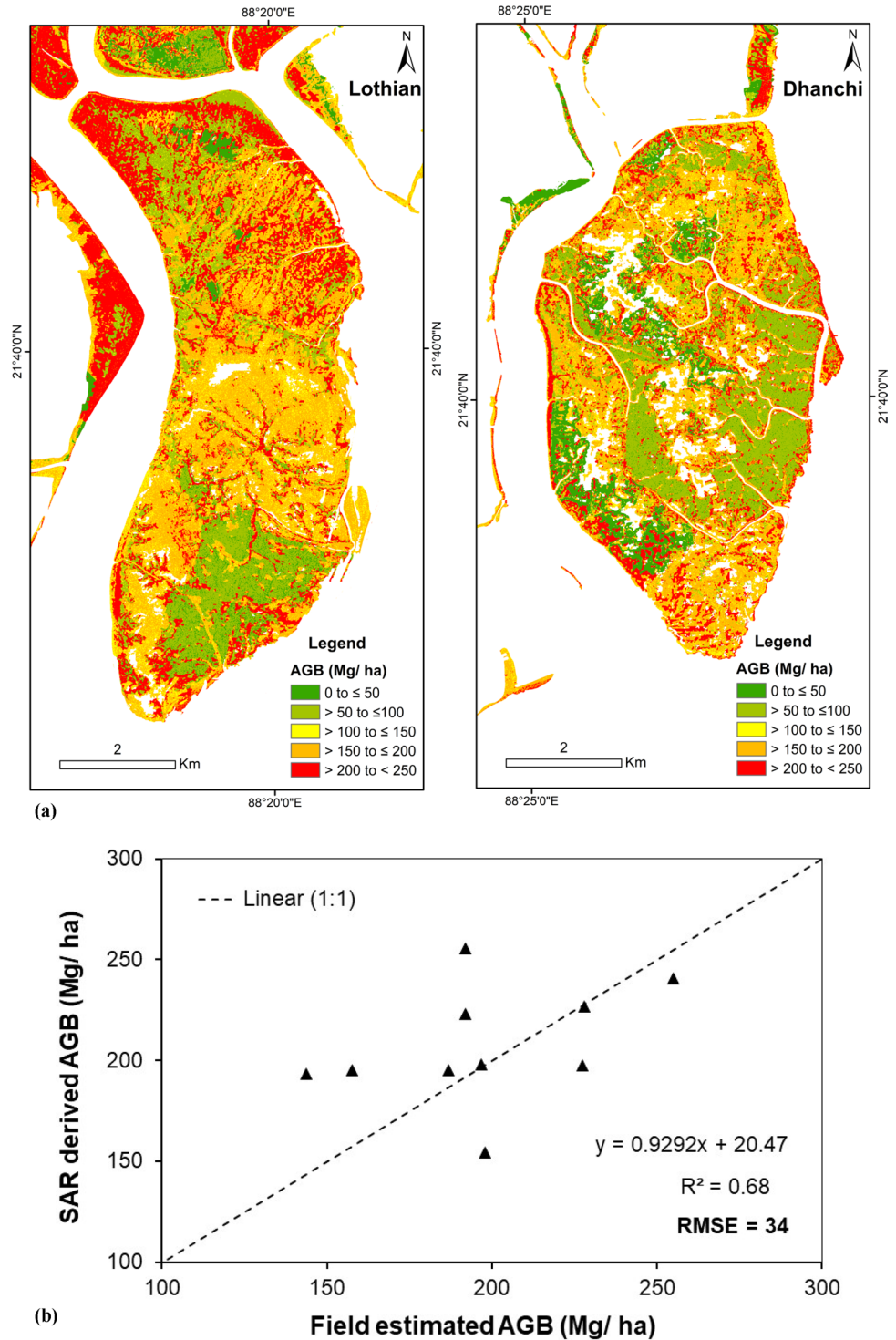
**Fig. 8** Field photographs of dense (a, b) and sparse mangrove (c, d)



1.6963 dB, that at maximum foliage was found to be  $-4.9980$  dB with a standard deviation of 1.7923 dB and that at leaf off was found to be  $-8.4729$  dB with a standard deviation of 1.7121 dB. Sigma naught was increased by an average of 4.992 dB from leaf onset to maximum foliage and then reduced by an average of 3.4749 dB from maximum foliage to leaf offset. The date for leaf onset on average was found to

be 6 May 2022 with a standard deviation of 26.37 days, for maximum foliage it was found to be 28 August 2022 with a standard deviation of 23.06 days, and for leaf offset, it was found to be 9 November 2022 with a standard deviation of 22.05 days (Table 3). This period between leaf onset and leaf offset during which the trees are most photosynthetically active was found on average to be about 187 days.

**Fig. 9** **a** SAR-derived above-ground biomass of mangrove area (excluding saline blanks) of the two islands. **b** Correlation between SAR-derived and field-estimated aboveground biomass



## Mangrove Characterization Study

The mangrove forests of the two islands could be classified into two broad classes, viz. dense mangrove (forests having  $> 40\%$  of canopy closure) and sparse mangrove (areas having  $< 40\%$  canopy closure) (Fig. 7). XPR values were  $> 1$  and  $\leq 1.6$  in sparse mangrove, while values were  $> 1.6$  and  $< 1.8$  in dense mangrove. Some of the field photographs are given in Fig. 8.

The mangrove forests in the study area could be classified broadly into 3 classes based on homogeneity/heterogeneity, viz. Class 1: highly heterogeneous, Class 2: moderate and Class 3: highly homogeneous (Fig. 7). Class 1 was characterized by high E and low ASM values ( $0.01\text{--}0.06$  ASM and  $3\text{--}4.7$  E). Class 2 showed moderate/intermediate values of both ASM and E ( $> 0.06\text{--}0.10$  ASM and  $2.7\text{--}< 3$  E), while Class 3 exhibited low E and high ASM values ( $> 0.10\text{--}0.23$  ASM and  $1.1\text{--}< 2.7$  E).

SAR-derived estimates were obtained over the two islands (Fig. 9). The mean AGB calculated was  $151$  Mg/ha and the values ranged from  $29$  to  $241$  Mg/ha. The ranges of AGB values were  $180\text{--}241$  Mg/ha in *Avicennia* communities,  $47\text{--}148$  Mg/ha in *Aegialitis-Excoecaria* communities,  $153\text{--}237$  Mg/ha in *Excoecaria* patches,  $78\text{--}105$  in mixed (*Ceriops-Excoecaria-Phoenix*) patches,  $108\text{--}233$  Mg/ha in mixed mangroves,  $102\text{--}229$  Mg/ha in fringe mangrove and  $29\text{--}106$  Mg/ha in *Phoenix* communities. The validation root mean square error (RMSE) was calculated to be  $34$  Mg/ha. Figure 9b shows the correlation between the SAR-derived and the field-estimated AGB values.

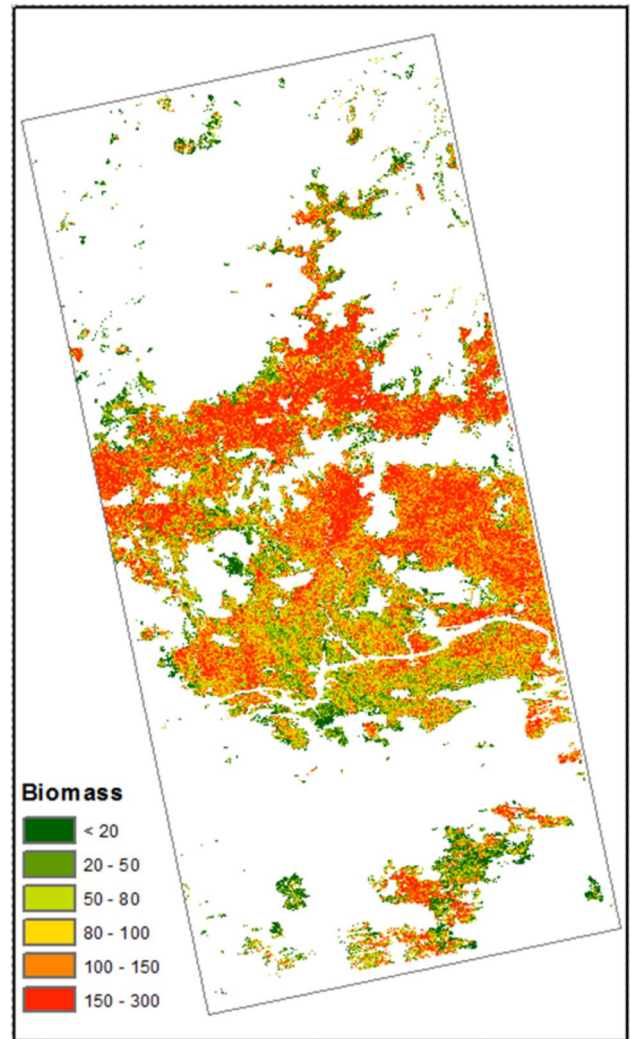


**Fig. 11** Forest AGB map estimated through EOS-04 C-band and ALOS PALSAR L-band data

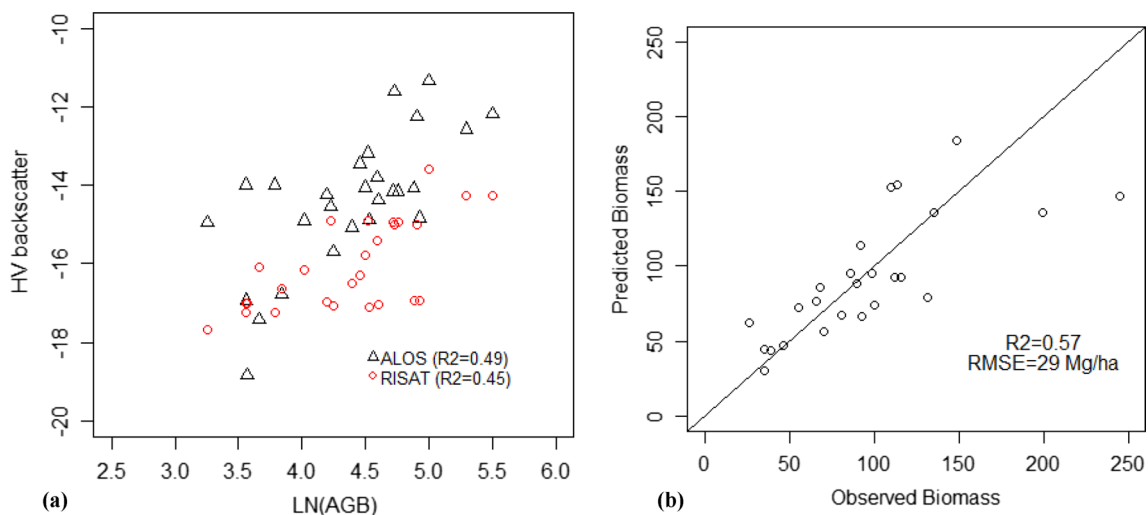


**Fig. 10** **a** Correlation between SAR backscatter and log (biomass), **b** correlation between observed and model-predicted biomass

## Forest Aboveground Biomass Upscaling

In this study, C- and L-band data were explored for forest biomass estimation using field inventory data from 26 plots of 0.1 ha size. Field-measured biomass values in the site varied from 26 to 244 Mg/ha. C-band HV backscatter gave a correlation coefficient of 0.45 which is hindered mainly due to saturation in high biomass in the area. Same field inventory data were also correlated with L-band SAR data ALOS PALSAR which gave a correlation coefficient of 0.49. It is observed that C-band data gave better correlation in the low-biomass regions. However, the L-band gave better separation in the medium–high-biomass region (Fig. 10a). Field inventory was carried out during 2019 which lead to the time difference of nearly 3 years with EOS04 data. However, L-band data from ALOS PALSAR-2 were used from the same year (2019). The time difference between field inventory and EOS04 data could also be one of the attributes for higher uncertainty in the biomass estimation using C-band EOS04 data. The future course of work will include concurrent field inventory data to enhance AGB mapping. Finally, a combination of C- and L-band data was used to spatially estimate the biomass which gave a correlation coefficient of 0.57 with an estimation error of 29 Mg/ha (Figs. 10b, 11).

C-band correlation equation (EOS04):

$$\text{Log}(\text{biomass}) = 0.292 * \text{HV}_{c\text{-band}} + 9.0352 \quad (6)$$

L-band correlation equation (ALOS PALSAR-2):

$$\text{Log}(\text{biomass}) = 0.2417 \times \text{HV}_{l\text{-band}} + 7.8873 \quad (7)$$

C- and L-band multiple regression:

$$\text{Log}(\text{biomass}) = 0.1999 \times \text{HV}_{l\text{-band}} + 0.0887 \times \text{HV}_{c\text{-band}} + 8.6911 \quad (8)$$

A similar analysis was carried out in a low-biomass site in the part of southern Rajasthan which covered in low-biomass regions with field-measured biomass values ranging from 10 to 121 Mg/ha. HV backscatter in this region could estimate the biomass with a correlation coefficient of 0.62.

## Discussion

### Land Surface Phenology Tracking Study

In the present, we could see that not all of the forest enters the leaf onset (Fig. 6d), achieves maximum foliage (Fig. 6e) and enters leaf offset (Fig. 6f) at the same time. These variations in land surface phenology can be due to different species composition, microclimatic conditions, terrain and soil conditions. A spatial description of land surface phenology as described by derived phenological metrics can be used to

study the effect these internal and external factors have on phenological metrics.

Forest phenology as tracked using EOS-04 datasets or by Sentinel-1 satellites (Soudani et al., 2021) reduces the need of field-based tracking of such event. Systematic acquisitions from EOS-04 data have made such tracking possible. Forest phenology has been identified as an important indicator of climate change (Tiwari et al., 2021). Long-term systematic acquisition from EOS-04 will be used to track changes in phenological metrics over many years and will be used to quantify the effects of climate change of forests.

Land surface phenology as tracked at medium to high resolution can be used for mapping of forest tree species or tree communities (Kurian et al., 2022). Complete land surface phenology from EOS-04 datasets as compared to multi-spectral index-based land surface phenology can be helpful in improving the results of such studies (Kurian et al., 2022).

## Mangrove Characterization Study

### Density-Level Classification of Mangrove Canopy

Dense mangrove (Figs. 7a, b and 8) corresponded to very dense and moderately dense forests, while sparse mangrove depicted sparse and open forest zones of the forest cover classification scheme provided by FSI. Kumar and Patnaik (2013) have used dual polarization (HH, HV) RADARSAT-2 datasets to characterize and discriminate mangrove forests of the Sundarbans biosphere reserve. A decision rule-based classification was applied on a combination of three-date HH with the single-date cross-polarization ratio for discriminating mangrove forests from other types of land-cover classes. However, in this study canopy density classification was not performed. Verghese et al. (2016) evaluated the feasibility of different polarimetric SAR data decomposition methods in canopy density classification of dry deciduous forests of Madhav National Park, India, using fully polarimetric C-band SAR data of RADARSAT-2.

### Classification of the Mangroves Based on Canopy Homogeneity/Heterogeneity

Class 1 (Fig. 7c, d) exhibited areas fringing the islands and along the creeks, while Class 3 exhibited mangrove areas of the ridge region. Chakraborty et al. (2013) demonstrated the great potential for using Radar Imaging Satellite-1 (RISAT-1) C-band SAR for discriminating mangroves from adjoining land covers, but in this study use of texture measures was not attempted. GLCM texture measures: contrast, entropy, correlation and variance were used on Sentinel 1 time series

SAR data for discriminating certain agricultural crops in the Bonaerense valley in the Villarino district of Buenos Aires Province, Argentina (Caballero et al., 2020).

### SAR-Derived Aboveground Biomass of Mangroves

In the present study, the AGB values ranged from 29 to 241 Mg/ha. Ghosh and Behera (2021) reported AGB values ranging from 70 to 666 t/ha using Sentinel 1A data of 2018 for mangroves of Bhitarkanika Wildlife Sanctuary, Odisha. Likewise, the AGB values ranged from 0.10 to 213 Mg/ha using Sentinel 1A images of 2018 over mangroves of Mundra taluka in the Kachch district of Gujarat (Vaghela et al., 2021). Pham et al. (2020) reported AGB ranging from less than 40 to 339.85 Mg/ha with a validation RMSE of 70.882 and  $R^2$  of 0.577 over mangroves of Ca Mau Province in Vietnam. The Sentinel 1A dataset's saturation level was exceeded by the mean AGB in this study, which could have led to an underestimation in the high AGB plots.

### Forest Aboveground Biomass Upscaling

SAR data with cloud penetration and all-weather capability along with sensitivity towards physical and geometrical properties of forest stands are being used for retrieval of biophysical parameters of forest like forest AGB, tree height, etc. SAR data have been used extensively for forest biomass estimation over Indian forest (Suresh et al., 2014; Thumaty et al., 2016); however, there are not many studies which utilizes different frequencies together for forest biomass estimation. In this study, we have demonstrated that C-band EOS-04 data can be used for mapping AGB of low to medium regions and how it can be effectively combined with L-band datasets for better accuracies. SAR backscatter in cross-polarization is strongly correlated with forest AGB due to volumetric scattering with forest stands. It is observed that C-band HV backscatter is strongly correlated with AGB in low–medium-biomass ranges. HV backscatter from C- and L-band estimates AGB with correlation coefficient of 0.45 and 0.49 in the study area which further improves to 0.57 when C- and L-band used together to predict the AGB.

### Conclusion

In this study, we have demonstrated that systematic acquisition of MRS product by EOS-04 can be used to monitor land surface phenology (including during the monsoon season) and to derive various phenological metrics. Such studies will help to track the land surface phenology of the forests at

the time when the majority of the photosynthetic activity is occurring.

With EOS-04 C-band data, mangrove forests were easily classified into density classes, viz. dense and sparse mangrove. GLCM textures on EOS-04 data were used to characterize mangrove forests into 3 classes of homogeneity/heterogeneity. Mangrove community-wise AGB estimates were calculated using the dual polarization EOS-04 data. Such studies will be helpful in monitoring the biomass status of threatened mangrove ecosystems over time.

EOS-04 data were used to successfully estimate AGB in low-density biomass regions and in combination with L-band data in low- to medium-AGB regions. A combination of C-band and L-band data is capable of providing improved results as compared to the results of each individually. RISAT C-band data along with the upcoming NISAR mission will enable the synergistic utilization of C-, S- and L-band data for improved forest biomass and carbon reporting.

**Acknowledgements** The authors express their sincere gratitude to the Chief General Manager, Regional Centres, NRSC, for his technical support. The authors are also grateful to General Manager, RRSC-West Jodhpur, Deputy General Manager and Head (Applications), RRSC-East, Kolkata and Deputy General Manager, RRSC-North, for their support in carrying out the work. The authors are thankful to the Principal Chief Conservators of Forests (PCCFs), Director, Sundarban Biosphere Reserve and other officials of West Bengal Forest Department, for granting permissions for field visits in the forests.

**Author Contributions** All the author have contributed equally to this work.

**Funding** This research did not receive any specific grant from funding agencies in public, commercial or not-for-profit sectors.

### Declarations

**Conflict of interest** The authors declare that they have no conflict of interest.

### References

- Ajai, N. S., Tamilarasan, V., Chauhan, H. B., Bahuguna, A., Gupta, M. C., Rajawat, A. S., Chaudhury, N. R., Kumar, T., Rao, R. S., Bhattacharya, S., Ramakrishnan, R., Bhandari, R. J., Mahapatra, M., et al. (2012). Coastal zones of India. Space Applications Centre, Ahmedabad.
- Bonan, G. (2008). Forests and climate change: Forcings, feedbacks, and the climate benefits of forests. *Science*, 320(5882), 1444–1449.
- Briggs, S. V. (1977). Estimates of biomass in a temperate mangrove community. *Austral Ecology*, 2(3), 369–373. <https://doi.org/10.1111/j.1442-9993.1977.tb01151.x>
- Brown, T., Hultine, K., Steltzer, H., Denny, E., Denslow, M., Grados, J., Henderson, S., Moore, D., Nagai, S., Sanclements, M., Sanchez-Azofeifa, G. A., Sonnentag, O., Tazik, D., & Richardson, A. (2016). Using phenocams to monitor our changing Earth: Toward a global phenocam network. *Frontiers in Ecology and the Environment*, 14, 84–93. <https://doi.org/10.1002/fee.1222>

- Caballero, R. G., Platzeck, G., Pezzola, A., Casella, A., Winschel, C., Silva, S. S., Ludueña, E., Pasqualotto, N., & Delegido, J. (2020). Assessment of multi-date Sentinel-1 Polarizations and GLCM texture features capacity for onion and sunflower classification in an irrigated valley: An object level approach. *Agronomy*, 2020(10), 845. <https://doi.org/10.3390/agronomy10060845>
- Chakraborty, M., et al. (2013). Initial results using RISAT-1 C-band SAR data. *Current Science*, 104, 490–501.
- Clausi, D. A. (2002). An analysis of co-occurrence texture statistics as a function of grey level quantization. *Canadian Journal of Remote Sensing*, 28, 45–62. <https://doi.org/10.5589/m02-004>
- FAO and UNEP. (2020). *The State of the World's Forests 2020. Forests, biodiversity and people*. <https://doi.org/10.4060/ca8642en>
- FRI. (1996). *Indian woods: Their identification, properties and uses. Volume I-VI*. Forest Research Institute, Ministry of Environment and Forests.
- FSI. (1996). *Volume equations for forests of India, Nepal and Bhutan Forest Survey of India*. Ministry of Environment and Forests, Govt. of India
- Garg, R. D., Agarwal, S., & Dadhwal, V. (2008). Evaluation of approaches for AWiFS multi-date registration. *International Journal of Applied Earth Observation and Geoinformation*, 10, 175–180. <https://doi.org/10.1016/j.jag.2008.02.011>
- Ghosh, S. M., & Behera, M. D. (2021). Aboveground biomass estimates of tropical mangrove forest using Sentinel-1 SAR coherence data—The superiority of deep learning over a semi-empirical model. *Computers and Geosciences*. <https://doi.org/10.1016/j.cageo.2021.104737>
- Gibbs, H. K., Brown, S., Niles, J. O., & Foley, J. A. (2007). Monitoring and estimating tropical forest carbon stocks: Making REDD a reality. *Environmental Research Letters*, 2(4), 045023. <https://doi.org/10.1088/1748-9326/2/4/045023>
- Hayashi, M., Motohka, T., & Sawada, Y. (2019). Aboveground biomass mapping using ALOS-2/PALSAR-2 time-series images for Borneo's Forest. *IEEE Journal of Selected Topics in Applied Earth Observations and Remote Sensing*, 12, 5167–5177. <https://doi.org/10.1109/JSTARS.2019.2957549>
- Ilic, J., Boland, D., McDonald, M., Downes, G., & Blakemore, P. (2000). *Woody density phase 1—State of knowledge*. National carbon accounting system, Technical Report 18. Australian Greenhouse Office.
- Joshi, H., & Ghose, M. (2014). Community structure, species diversity, and aboveground biomass of the Sundarbans mangrove swamps. *Tropical Ecology*, 55, 283–303.
- Kaul, M., Mohren, G. M. J., & Dadhwal, V. K. (2011). Phytomass carbon pool of trees and forests in India. *Climate Change*, 108, 243–259.
- Kumar, T., Das, P. K., Chandrasekar, K., Bandyopadhyay, S., & Dutta, D. (2021). *Characterization of Indian Sundarban mangroves using airborne multi-configuration SAR data and ground observations*. NRSC-RRSC-KOLK-Sep 2021-TR0001903-V1.0
- Kumar, T., & Patnaik, C. (2013). Discrimination of mangrove forests and characterization of adjoining land cover classes using temporal C-band Synthetic Aperture Radar data: A case study of Sundarbans. *International Journal of Applied Earth Observation and Geoinformation*, 23, 119–131.
- Kurian, A., Naveen, B. K., Reddy, C. S., Mayamanikandan, T., Narayanan, B., Debabrata, B., & Narayanan, A. (2022). Remote sensing based characterisation of community level phenological variations in a regional forest landscape of Western Ghats, India. *Geocarto International*, 37(27), 16620–16635. <https://doi.org/10.1080/10106049.2022.2112304>
- Lechner, A., Foody, G. M., & Boyd, D. S. (2020). Applications in remote sensing to forest ecology and management. *One Earth*, 2, 405–412. <https://doi.org/10.1016/j.oneear.2020.05.001>
- Martawijaya, A. (1992). *Indonesian Wood Atlas Vol. I. and II*. Department of Forestry, Agency for Forestry Research and Development, Forest Products Research and Development Centre.
- Mas, J., & Araújo, F. (2021). Assessing landsat images availability and its effects on phenological metrics. *Forests*, 12, 574. <https://doi.org/10.3390/f12050574>
- Mermoz, S., Réjou-Méchain, M., Villard, L., Le Toan, T., Rossi, V., & Gourlet-Fleury, S. (2015). Decrease of L-band SAR backscatter with biomass of dense forests. *Remote Sensing of Environment*, 159, 307–317. <https://doi.org/10.1016/j.rse.2014.12.019>
- Mishra, A. P., Rai, I. D., Pangtey, D., & Padalia, H. (2021). Vegetation characterization at community level using Sentinel-2 satellite data and random forest classifier in Western Himalayan Foothills, Uttarakhand. *Journal of the Indian Society of Remote Sensing*, 49, 759–771. <https://doi.org/10.1007/s12524-020-01253-x>
- Misra, G., Cawkwell, F., & Wingler, A. (2020). Status of phenological research using Sentinel-2 data: A review. *Remote Sensing*, 12, 2760. <https://doi.org/10.3390/rs12172760>
- Nelson, M. D., Ward, K. T., & Marvin, E. B. (2006). Forest-cover-type separation using RADARSAT-1 synthetic aperture radar imagery. In *Proceedings of the 8th annual forest inventory and analysis symposium* (pp. 303–306).
- Peebles, P. Z., Jr. (1998). *Radar principles* (p. 20). Wiley.
- Pham, M. H., Do, T. H., Pham, V.-M., & Bui, Q.-T. (2020). Mangrove forest classification and aboveground biomass estimation using an atom search algorithm and adaptive neurofuzzy inference system. *PLoS ONE*. <https://doi.org/10.1371/journal.pone.0233110>
- Proisy, C., Mougin, E., & Fromard, F. (2001). Radar remote sensing of mangroves: Results and perspectives. In *Proceedings of IGARSS conference*, Sydney, Australia, 9–13 July 2001.
- Rajashekar, G., Fararoda, R., Reddy, R. S., Jha, C. S., Ganeshaiyah, K. N., Singh, J. S., & Dadhwal, V. K. (2018). Spatial distribution of forest biomass carbon (Above and below ground) in Indian forests. *Ecological Indicators*, 85, 742–752. <https://doi.org/10.1016/j.ecoli.2017.11.024>
- Rakesh, F., Reddy, R. S., Rajashekar, G., Chand, T. K., Jha, C. S., & Dadhwal, V. K. (2021). Improving forest above ground biomass estimates over Indian forests using multi source data sets with machine learning algorithm. *Ecological Informatics*, 65, 101392. <https://doi.org/10.1016/j.ecoinf.2021.101392>
- Reddy, C. S., Jha, C. S., Diwakar, P. G., & Dadhwal, V. K. (2015). Nationwide classification of forest types of India using remote sensing and GIS. *Environmental Monitoring and Assessment*, 187(12), 777. <https://doi.org/10.1007/s10661-015-4990-8>
- Reddy, R. S., Rajashekar, G., Jha, C. S., Dadhwal, V. K., Pelissier, R., & Coueron, P. (2017). Estimation of above ground biomass using texture metrics derived from IRS Cartosat-1 panchromatic data in evergreen forests of Western Ghats, India. *Journal of the Indian Society of Remote Sensing*, 45(4), 657–665. <https://doi.org/10.1007/s12524-016-0630-1>
- Richardson, A. D., Black, T. A., Ciais, P., Delbart, N., Friedl, M. A., Gobron, N., Hollinger, D. Y., Kutsch, W. L., Longdoz, B., Luysaert, S., Migliavacca, M., Montagnani, L., Munger, J. W., Moors, E., Piao, S., Rebmann, C., Reichstein, M., Saigusa, N., Tomelleri, E., ... Varlagin, A. (2010). Influence of spring and autumn phenological transitions on forest ecosystem productivity. *Philosophical Transactions of the Royal Society B: Biological Sciences*, 365, 3227–3246. <https://doi.org/10.1098/rstb.2010.0102>
- Schaber, J., & Bodeck, F.-W. (2002). Evaluation of methods for the combination of phenological time series and outlier detection. *Tree Physiology*, 22, 973–982. <https://doi.org/10.1093/treephys/22.14.973>
- Solomon, S. (2007). *Climate change 2007—The physical science basis: Working group I contribution to the fourth assessment report of the IPCC*. Cambridge University Press.

- Soudani, K., Delpierre, N., Berveiller, D., Hmimina, G., Pontailier, J.-Y., Seureau, L., Vincent, G., & Dufrêne, É. (2021). A survey of proximal methods for monitoring leaf phenology in temperate deciduous forests. *Biogeosciences*, *18*, 3391–3408. <https://doi.org/10.5194/bg-18-3391-2021>
- Suresh, M., Chand, T. K., Fararoda, R., Jha, C. S., & Dadhwal, V. K. (2014). Forest above ground biomass estimation and forest/non-forest classification for Odisha, India, using L-band Synthetic Aperture Radar (SAR) data. *The International Archives of the Photogrammetry, Remote Sensing and Spatial Information Sciences*, 651–658.
- Thumaty, K. C., Fararoda, R., Middinti, S., Gopalakrishnan, R., Jha, C. S., & Dadhwal, V. K. (2016). Estimation of above ground biomass for central Indian deciduous forests using ALOS PALSAR L-band data. *Journal of the Indian Society of Remote Sensing*, *44*(1), 31–39. <https://doi.org/10.1007/s12524-015-0462-4>
- Tiwari, P., Verma, P., & Raghubanshi, A. (2021). Forest phenology as an indicator of climate change: Impact and mitigation strategies in India. <https://doi.org/10.1007/978-3-030-67865-4>
- Vaghela, B., Chirakkal, S., Putrevu, D., & Solanki, H. (2021). Modeling above ground biomass of Indian mangrove forest using dual-pol SAR data. *Remote Sensing Applications: Society and Environment*. <https://doi.org/10.1016/j.rsase.2020.100457>
- Verghese, A.O., Suryavanshi, A., & Joshi, A. K. (2016). Analysis of different polarimetric target decomposition methods in forest density classification using C band SAR data. *International Journal of Remote Sensing*, *37*(3). <https://doi.org/10.1080/01431161.2015.1136448>.
- Wang, Y., Hess, L. L., Filoso, S., & Melack, J. M. (1995). Understanding the radar backscattering from flooded and non-flooded Amazon forests: Results from canopy backscatter modeling. *Remote Sensing of Environment*, *54*, 324–332. [https://doi.org/10.1016/0034-4257\(95\)00140-9](https://doi.org/10.1016/0034-4257(95)00140-9)
- Wani, S. P., Chander, G., Sahrawat, K. L., Rao, C. S., Raghvendra, G., Susanna, P., & Pavani, M. (2012). Carbon sequestration and land rehabilitation through *Jatropha curcas* (L.) plantation in degraded lands. *Agriculture, Ecosystems & Environment*, *161*, 112–120. <https://doi.org/10.1016/j.agee.2012.07.028>
- Zhang, X., Liu, L., Liu, Y., Senthilnath, J., Wang, J., Moon, M., Hennebry, G., Friedl, M., & Schaaf, C. (2018). Generation and evaluation of the VIIRS land surface phenology product. *Remote Sensing of Environment*. <https://doi.org/10.1016/j.rse.2018.06.047>

**Publisher's Note** Springer Nature remains neutral with regard to jurisdictional claims in published maps and institutional affiliations.

Springer Nature or its licensor (e.g. a society or other partner) holds exclusive rights to this article under a publishing agreement with the author(s) or other rightsholder(s); author self-archiving of the accepted manuscript version of this article is solely governed by the terms of such publishing agreement and applicable law.